Multicomponent aluminum composites Al – Cr – Zr, Al – Cr – Zr – Co – Ti – Cu with small additions of nanoparticles of refractory compounds SiC or $MgAl_2O_4$: thermochemistry, structure and properties

L. E. Agureev, *Candidate of Technical Sciences, Leading Researcher at the Nanotechnology Department*[1, 2], *e-mail: trynano@gmail.com*
S. V. Savushkina, *Doctor of Technical Sciences, Professor, Researcher at the Nanotechnology Department*[1, 2]
G. V. Belov, *Doctor of Technical Sciences, Leading Researcher*[3]
M. A. Lyakhovetsky, *Candidate of Technical Sciences, Associate Professor, Leading Researcher*[1], *e-mail: maxim.lyakhovetskiy@mai.ru*

[1]*Moscow Aviation Institute, Moscow, Russia.*
[2]*Keldysh Research Center, Moscow, Russia.*
[3]*Bauman Moscow State Technical University, Moscow, Russia.*

The ability to increase the operating temperature of powder aluminum matrix composites by introducing alloying metals (Zr, Cr, Co, Ti, and Cu) and nanoparticles of refractory substances has been studied. The equilibrium composition of the Al – Cr – Zr – Co – Ti – Cu system has been calculated using contemporary modeling techniques for equilibrium processes (jmatro® and HSC®). Calculations indicate the presence of Al, Al_3M ($D0_{23}$), Al_7Cr, Al_7Cu_2M, and Al_9M_2 phases in aluminum at the sintering temperature, where M is an additive metal. Gibbs energies and equilibrium constants for the formation of intermetallic compounds have been calculated. The intensification of the solid-phase reaction between aluminium and silicon carbide is contingent upon the presence of free carbon within the system Al – Cr – Zr – Co – Ti – Cu evidenced by calculations of the Gibbs energy and equilibrium constant. An aluminum composite Al – Cr – Zr – Co – Ti – Cu modified with SiC and $MgAl_2O_4$ nanoparticles has been produced through mechanical alloying, hydrostatic pressing, and spark plasma sintering. The next materials were prepared: Al – 0.5%Cr – 0.3%Zr, Al – 0.5%Cr – 0.3%Zr + 0.1% SiC, Al – 0.5%Cr – 0.3%Zr + + 0.1 $MgAl_2O_4$, Al – 0.5%Cr – 0.25%Zr – 0.2%Co – 0.2%Ti – 0.2%Cu, Al – 0.5%Cr – 0.25 Zr – 0.2%Co – 0.2%Ti – – 0.2%Cu + 0.1%SiC, Al – 0.5%Cr – 0.25%Zr – 0.2%Co – 0.2%Ti – 0.2%Cu + 0.1%$MgAl_2O_4$. The microstructure of the samples was analyzed. It was found that the segmentation effect, in which a large inclusion splits into smaller grains, is linked to the formation of intermetallic compounds with different crystalline structures, compositions and stoichiometry. The bending strength and Young's modulus at different temperatures for Al – Cr – Zr and Al – Cr – Zr – Co – Ti – Cu materials, as well as those modified with aluminum-magnesium spinel and silicon carbide nanoparticles, were measured. The material exhibits high bending strength at 400 °C (up to 191 MPa).

Key words: aluminum composites, nanoparticles, spark plasma sintering, thermodynamic modelling, bending strength, Young's modulus

DOI: 10.17580/nfm.2025.01.03

Introduction

Application of Al composites

The use of powder aluminium composites as a structural material is a promising due to their low weight, low capital costs for production, and most importantly, high specific strength. However, their use is confined to applications that not necessitate substantial wear resistance and elevated operating temperatures. In this work the ability to elevate the operational temperature of powder aluminium matrix composites through the incorporation of alloying additives of metals (Zr, Cr, Co, Ti, and Cu) and nanoparticles of refractory substances in small quantities was studied. It is anticipated that these materials will be employed to enhance the service life and operational efficiency of a range of mechanical engineering units, including engine impellers, gear wheels, bushings, spacers and so forth. This is expected to be achieved even when these materials are subjected to conditions of exposure to aggressive oxidizing gaseous or liquid media.

Microalloying and the influence of additives on aluminum

It is established that at elevated temperatures, aluminium alloys undergo a loss of thermal stability, accompanied by the growth of grains, primary crystals, impurities, and transformations, as well as the growth of intermetallic coarse phases and spheroidization [1]. This ultimately results in a deterioration of the high-temperature mechanical and functional properties of aluminium.

Nevertheless, the incorporation of transition metals into the matrix can serve to counteract these detrimental effects. The material obtained by spark plasma sintering (SPS) based on the Al – Cr – Zr system has demonstrated favourable mechanical properties. The total concentration of chromium and zirconium did not exceed 0.8 wt.% in one instance [2], while in another case, it reached 3.6 wt. % [3]. This is due to the formation of intermetallic phases of nano- and submicron size in aluminium by chromium and zirconium resulted in enhanced strength. Typically, these are Al_3Zr and Al_7Cr. However, in rapidly cooled alloys, a supersaturated solid solution of the transition metal in aluminium is also present. In spark plasma sintered aluminium strengthening mechanisms associated with fine grain and precipitation of intermetallic nanosized phases operate together. In this study, we investigated the effect of titanium, cobalt and copper additives on a similar material, which also contains chromium and zirconium, but the thickness of the sintered samples was 30% greater.

The addition of even a small quantity of Zr (0.1%) to aluminium results in a notable enhancement in resistance to high-temperature creep. Furthermore, the combined addition of zirconium and chromium to aluminium enhances the processability and corrosion resistance of alloys. Trialuminides of transition metals have a high melting point, low density and resistance to oxidation. $TiAl_3$ has a $D0_{22}$ lattice [4, 5], while $ZrAl_3$ crystallize in $D0_{23}$ type. Additionally, the metastable phases of $TiAl_3$ and $ZrAl_3$ have an L_{12} lattice [6], which is preferable to matrix strengthening.

The enhancement of aluminium characteristics through the incorporation of transition metals can be achieved upon the prevention of primary coarse aluminide formation [7]. As evidenced by numerous studies [8–12], the coherence of Al_3Zr dispersoids with aluminum can be enhanced by the introduction of titanium additives. In a previous study [2], we demonstrated that the introduction of small quantities of chromium and zirconium into spark plasma sintered aluminium yielded highly favorable outcomes.

It is established that the addition of copper to aluminium results in the promotion of solid-solution and dispersion strengthening, although this process is accompanied by a reduction in corrosion resistance. It is therefore necessary to limit the quantity of copper introduced into aluminium to a level well below its solubility limit. As a consequence of the heat treatment and ageing of hardened aluminium-copper materials, secondary precipitates of metastable phases (dispersoids) are formed from a solid solution. These phases have a similar composition but differ in structure from the stable phases. This leads to a significant increase in strength. The principal strengthening phase of aluminium in the Al – Cu system is θ'-$CuAl_2$. The small dimensions of the blanks formed during SPS sintering, coupled with the elevated processing rates, including those resulting from electrodiffusion and relatively high heating and cooling rates, facilitate the attainment of a specific structure and composition of alloyed aluminium. In addition, during SPS sintering, the blank undergoes significant deformation contributed to the strengthening of aluminum by the deformation mechanism.

Among the intermetallics in the Al – Co system, Al_9Co_2 and $Al_{13}Co_4$ exhibit distinctive properties. Al_9Co_2 due to its unique electronic structure has enhanced corrosion resistance compared to conventional alloys [13].

It is established that the binary Al – Ti system comprises seven intermetallic compounds: $Ti_3Al(\alpha_2)$, $TiAl(\gamma)$, Ti_3Al_5, $TiAl_2(\eta)$, $Ti_2Al_5(\theta)$, $TiAl_3(h)$ and $TiAl_3(l)$ [14]. The most stable intermetallic phases enhanced the physical and mechanical properties of titanium aluminide are γ-TiAl, α_2-Ti_3Al and γ-TiAl + α_2-Ti_3Al [15–17]. On occasion, modern diagrams of binary alloys of the titanium-aluminum system contain not only the four established phases $\alpha_2(Ti_3Al)$, $\gamma(TiAl)$, $TiAl_2$ and $TiAl_3$, but also Ti_5Al_{11}, Ti_2Al_5.

In the binary system Al – Zr, ten intermetallic compounds have been identified, namely Zr_3Al, Zr_2Al, Zr_5Al_3, Zr_3Al_2, Zr_4Al_3, Zr_5Al_4, ZrAl, Zr_2Al_3, $ZrAl_2$ and $ZrAl_3$. The intermetallic compounds present in the Al – Co system are as follows: Al_9Co_2; $Al_{13}Co_4$; $Al_{13}Co_4$; $Al_{13}Co_4$; Al_3Co; Al_5Co_2; AlCo. [18, 19]. Concurrently, as indicated in [20], the solubility of chromium, titanium, zirconium and cobalt in aluminium is, respectively, 0.9%, 0.26%, 0.28% and 0.02%. The most stable phases are Al_7Cr, Al_3Ti, Al_3Zr and Al_9Co_2.

The introduction of small additives of nanoparticles of refractory compounds into aluminum can significantly improve its functional and strength properties [22, 23]. It should be noted that heating to higher temperatures is possible when spark plasma sintered aluminum at a temperature below its melting point. Aluminium-magnesium spinel particles are insoluble in aluminium. The interaction of silicon carbide particles with the aluminium matrix can result in the formation of free silicon and aluminium carbide. Furthermore, the presence of oxygen can facilitate the formation of aluminium oxycarbides. To ascertain the potential for such an interaction, calculations were conducted to determine the composition and change in Gibbs energy of the corresponding reactions as a function of temperature.

Thermodynamic modeling

A series of calculations were conducted in order to evaluate the impact of temperature on the phase composition of the resulting aluminium-based material. Initially, calculations were conducted in JmatPro® (v. 7.0) [24, 25] to determine the impact of temperature on the material composition. The changes in the standard Gibbs energy of dispersoid phases formation with the most probable stoichiometric composition were calculated using the HSC® software (ver. 9.0).

The results of the modelling conducted in the JmatPro® environment (ver. 7.0) with a database (Aluminium Alloys)

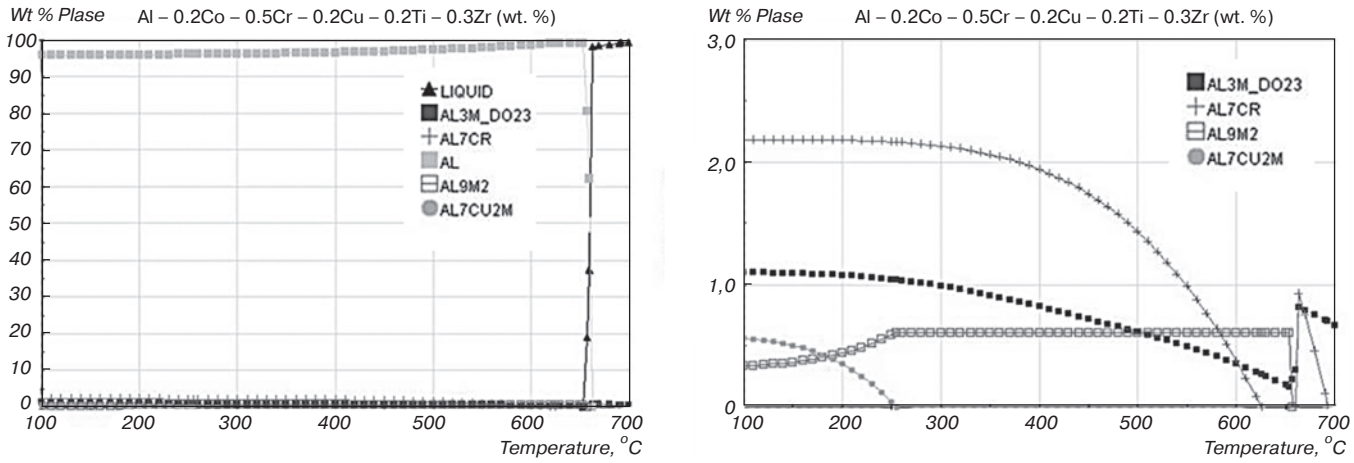

Fig. 1. Equilibrium composition vs. temperature calculated with JmatPro (v. 7.0)

of the temperature effect on the material composition are presented in **Fig. 1**. The calculations indicate the presence Al, Al_3M ($D0_{23}$), Al_7Cr, Al_7Cu_2M and Al_9M_2 phases in aluminium at the sintering temperature, where *M* is the additive metal.

It should be noted that the possibility of the AlTi intermetallic compound formation is relatively low in comparison to other intermetallic compounds presented in the system, particularly those with a lower titanium content. Furthermore, the formation of the titanium-depleted compound Al_2Ti is more thermodynamically probable [26]. According to [27], the intermetallic compound Al_2Ti with a smaller amount of aluminium can form during rapid quenching, despite the kinetic factors of resistance.

As demonstrated in [28–31], the addition of silicon carbide nanoparticles to aluminium can result in the formation of aluminium carbide even at temperatures significantly below the melting point of the metal. Furthermore, upon contact between liquid aluminium and silicon carbide, a solid solution of silicon in aluminium and free silicon are formed at the interphase boundary, in addition to aluminium carbide. The formation of Al_4C_3 proceeds as follows (1) [32]:

$$4\,[Al] + 3SiC_s \rightarrow Al_4C_{3s} + 3Si_s/[Si] \qquad (1)$$

It is established that the release of silicon from a supersaturated solid solution of aluminium occurs during rapid quenching, forming a eutectic with it or large primary crystals [33]. Nevertheless, this reaction is facilitated by the presence of liquid aluminium, with the selected sintering temperature being considerably lower than the melting point of aluminium. According to calculations in HSC® in the presence of free carbon the reaction of aluminium carbide formation with the release of free silicon also occurs in the solid phase **(Fig. 2)**. Free carbon can gain access to the sintered aluminium from graphite paper and punches utilized in the press molding process. Additionally, catalysis may occur during the decomposition of surfactants.

Materials and methods

The mechanical alloying of aluminium was conducted in an Activator-2SL planetary ball mill. Hardened steel balls with a diameter of 5 mm were employed for the grinding process in a ratio powder to balls 1:10. The following materials powders were employed: ASD-4, PH-1S, PTSR-1, PTOM-1, cobalt, PMU. A lubricant (HMDSZ) was added at a concentration of 0.1 wt.%. The mixing process was conducted for 30 minutes in argon environment within the Activator-2SL planetary mill. The samples were obtained via spark plasma sintering in an argon environment. In contrast to the samples described in reference [2], the resulting specimens were 3 mm thick, 30 mm in diameter, and in the form of flat tablets. The sintering process was conducted in graphite press molds with the use of graphite paper gaskets.

A nanoparticle concentration of 0.1 wt.% was selected for the additives in the composite materials. After drying, the powder mixture was compressed into graphite molds and spark plasma sintered. Subsequently, the samples were cut into rectangular blanks for further analysis. The next materials were formed: Al – 0.5%Cr – 0.3%Zr, Al – 0.5%Cr – 0.3%Zr + 0.1%SiC, Al – 0.5%Cr – 0.3%Zr + + 0.1%$MgAl_2O_4$, Al – 0.5%Cr – 0.25%Zr – 0.2%Co – 0.2%Ti – 0.2%Cu, Al – 0.5%Cr – 0.25%Zr – 0.2%Co – 0.2%Ti – 0.2%Cu + 0.1%SiC, Al – 0.5%Cr – 0.25%Zr – 0.2%Co – 0.2%Ti – 0.2%Cu + + 0.1%$MgAl_2O_4$.

The microstructure was studied using a FEI Quanta scanning electron microscope. The density and porosity of the samples were determined by hydrostatic weighing.

Porosity was determined for a sintered sample in the form of a tablet with a diameter of 30 mm and a height of 3 mm.

Thermomechanical properties of composite samples were investigated by TestSystems-VacETO high-temperature testing facility at temperatures ranging from 25 to 400 °C. The tests were conducted using a three-point bending method on samples in the form of rectangular

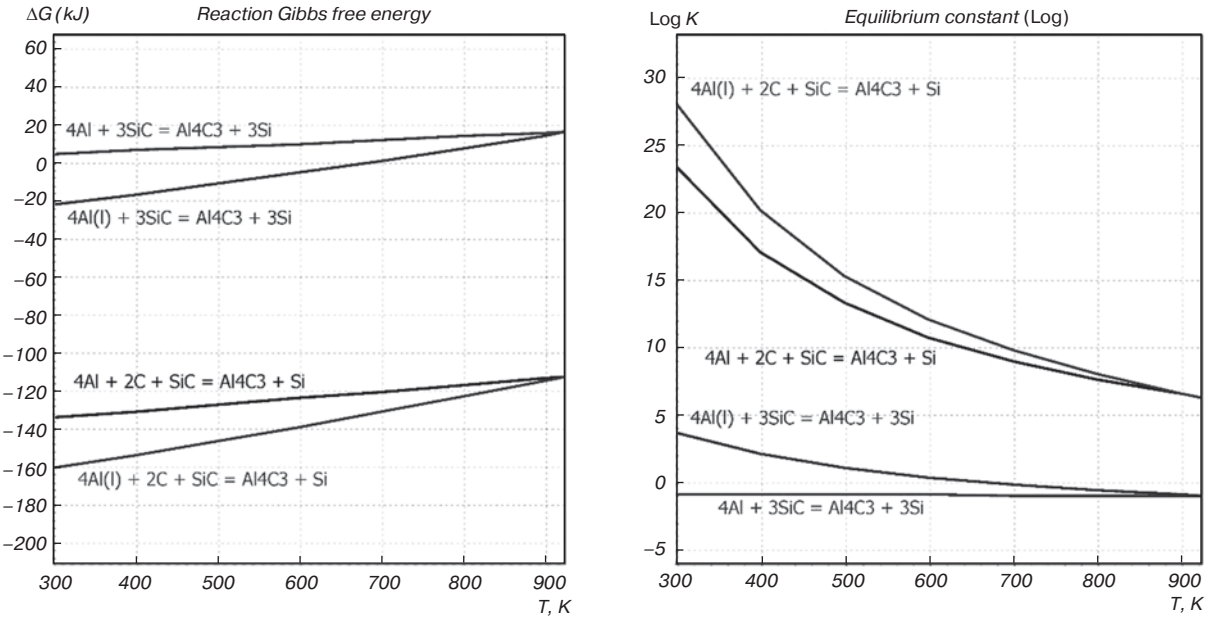

Fig. 2. Change in Gibbs energy and logarithm of equilibrium constant of aluminum carbide reactions formation

beams measuring 27 mm in length, 3 mm in width, and 3 mm in thickness.

Microstructure and phase composition

The addition of $MgAl_2O_4$ and SiC nanoparticles to Al – 0.5%Cr – 0.3%Zr – 0.2%Co – 0.2%Ti – 0.2%Cu alloys **(Fig. 3)** resulted in a notable reduction in the average grain size. The Al – 0.5%Cr – 0.25%Zr – 0.2%Co – 0.2%Ti – 0.2%Cu material is distinguished by the presence of individual, clearly delineated grains. Light precipitates of second phases of nano-, submicron, and micron sizes are visible inside and at the grain boundaries. The light inclusion of rounded shape is composed of multiple segments **(Fig. 3, *a*, *c*)**. At higher magnification, it becomes evident that these segments are composed of small grains of micron and submicron sizes **(Fig. 3, *b*, *d*)**. It can be assumed that this inclusion refers to chromium or reacted chromium, which is poorly ground due to high hardness and low grinding time. The segmentation effect, whereby a large inclusion divides into smaller grains, appears to be linked to the formation of intermetallic compounds with varying crystalline structures, compositions, and stoichiometries.

The grains of the aluminum matrix have regular, faceted shapes and are about a few micrometers in size. In the triple junctions of these grains, one can observe the presence of even smaller grains (less than 1 micrometer) of the matrix. Large white particles are most likely intermetallic phases of aluminum with

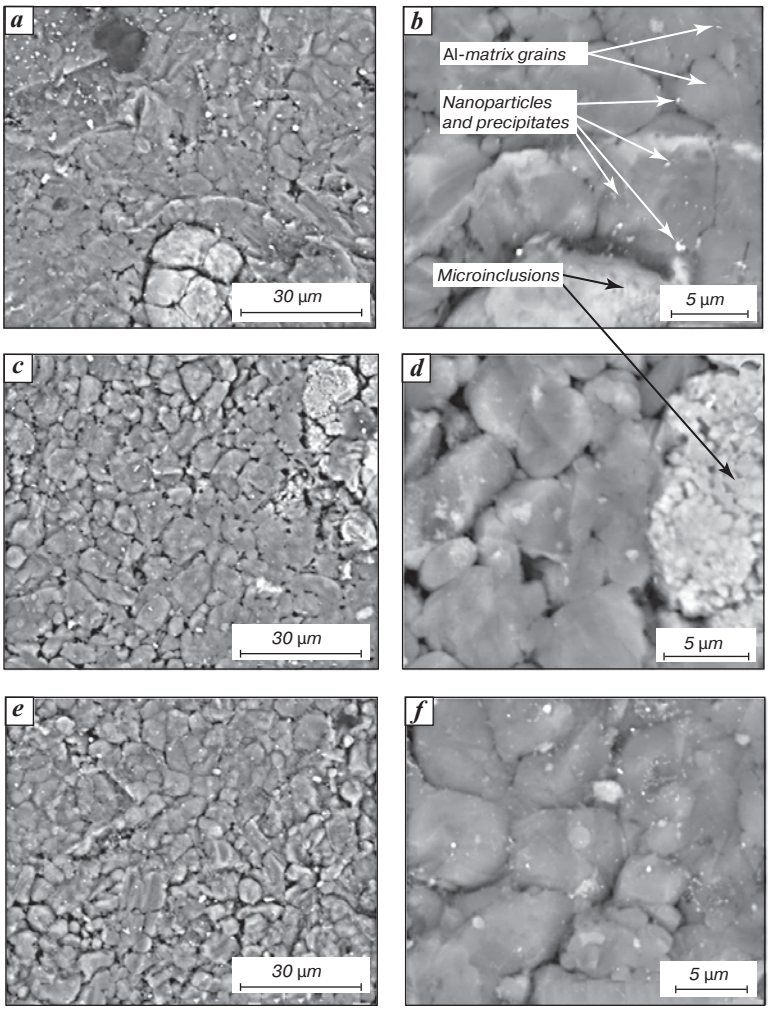

Fig. 3. Materials microstructure of the samples:
a, *b* – Al – 0.5%Cr – 0.3%Zr – 0.2%Co – 0.2%Ti – 0.2%Cu;
c, *d* – Al – 0.5%Cr – 0.3%Zr – 0.2%Co – 0.2%Ti – 0.2%Cu + + 0.1%$MgAl_2O_4$;
e, *f* – Al – 0.5%Cr – 0.3%Zr – 0.2%Co – 0.2%Ti – 0.2%Cu + 0.1% SiC

other transition metals, such as chromium, which have high hardness and may be difficult to grind. Nanoscale white phases, representing aluminum intermetallic compounds as well as high-temperature nanoparticles of additives, are also visible. Regularly shaped pores can be seen in the structure.

Phase analysis has been performed, and the results are shown in **Fig. 4**. The main phase is aluminum, as expected. Intermetallic phases are also present, but they have extremely weak reflections. Apparently, intermetallic phases exist in the material in the form of *X*-ray amorphous nanocrystals. In the diffraction patterns, the peaks corresponding to the approximate phases of Al_3Zr, Al_9Co_2, and Al_7Cr can be identified, which is in agreement with the results of thermodynamic modeling.

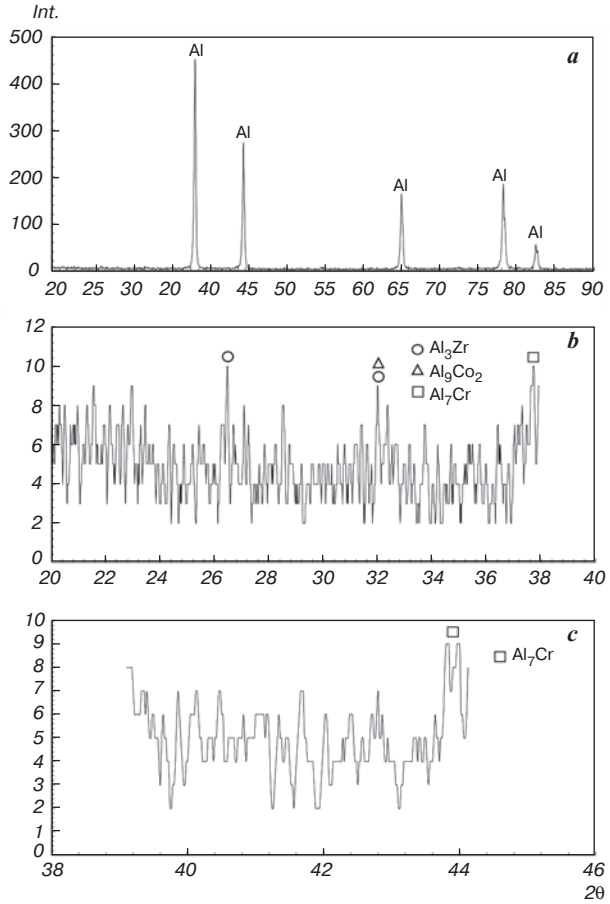

Fig. 4. XRD pattern of Al – Cr – Zr – Co – Ti – Cu material: *a* — overall plot, *b*, *c* — parts with intermetallic peaks

Properties

Table shows the changes in the modulus of elasticity and flexural strength of the Al – Cr–Zr, Al – Cr – Zr – Co – Ti – Cu, Al – Cr – Zr-nanoparticles, and Al – Cr – Zr – Co – Ti – Cu –nanoparticles composite samples at temperatures of 25, 200, 300, and 400 °C. It is noteworthy that the material modified with silicon carbide nanoparticles exhibits enhanced thermal stability in comparison to the material with aluminium magnesium spinel nanoparticles. This phenomenon is likely attributable to the dissolution of silicon carbide in aluminium. At temperatures below 300 °C, the highest flexural strength was demonstrated by the material Al – Cr – Zr – 0.6(Co,Ti,Cu) without ceramic nanoparticles. This may be attributed to the higher proportion of precipitates formed in aluminium compared to the Al – Cr – Zr material. Besides, nanoparticles introduced into the matrix ex-situ can form aggregates and introduce voids that weaken the material. The plasticity of the material is approximately 1.4–1.5%, and it does not vary significantly between samples.

The change in bending strength was found to be dependent on porosity, despite the different amounts and types of alloying components in the samples. In this case, it can be assumed that the addition of alloying components affects the internal structure of the sintered material. This is because insoluble nanoparticles tend to form agglomerates and subsequently introduce defects into the sintered material. However, the exact contribution of nanoparticles and intermetallic dispersoids remains unclear. A variety of factors contribute to the strength of alloys and metal composites, collectively referred to as strengthening mechanisms.

A wide range of research was conducted by the authors on the effect of adding small amounts of refractory nanoparticles to aluminum matrix materials in [34]. It was found that for the Al – 4Cu – $0.1Al_2O_3$ material sintered using the SPS method, the flexural strength at room tem-

Table
Change in the elastic modulus and change in the flexural strength of samples depending on temperature

Sample	Bending strength, MPa				Young's Modulus, GPa			
	25	200	300	400	25	200	300	400
Al + 0.5Cr + 0.3Zr	190	177	144	107	75	73	70	59
Al + 0.5Cr + 0.3Zr + 0.1$MgAl_2O_4$	200	181	150	113	63	62	61	55
Al + 0.5Cr + 0.3Zr + 0.1SiC	185	176	153	116	76	74	71	63
Al + 0.5Cr + 0.3Zr + 0.6(Co + Ti + Cu)	335	281	164	124	76	75	70	62
Al + 0.5Cr + 0.3Zr + 0.6(Co + Ti + Cu) + 0.1$MgAl_2O_4$	287	263	193	158	69	68	65	58
Al + 0.5Cr + 0.3Zr + 0.6(Co + Ti + Cu) + 0.1SiC	273	252	226	191	63	61	58	54

perature reached 310 MPa, which was 13% higher than that of pure aluminum. The flexural strength for aluminum with additions of transition metals, boron, and aluminum oxide nanoparticles was about 300 MPa and 120 MPa at 300 °C and room temperature (n.c.), respectively, according to work [35]. In [36], researchers studied the effect of a small amount of silicon carbide nanoparticles combined with boron carbide on alloy 6061 and achieved a tensile strength of 250 MPa at room temperature and ductility of up to 4%, using the SPS technique. Al – SiC composite materials were also prepared using the same technique, with increased carbide contents of 10%, 20%, and 30%, according to [28]. At the same time, the bending strength of the material with 20% silicon carbide increased by 47% to 331 MPa compared to the base material.

The addition of transition metals, such as cobalt, titanium, copper, as well as chromium and zirconium, to aluminum leads to the formation of high-temperature intermetallic compounds, including nanoscale structures. This contributes to an increase in strength, according to the Orowan mechanism, but significantly reduces ductility. During aluminum deformation, dislocations encounter numerous obstacles in the form of aluminum phases containing transition metals that are released during heat treatment. Despite this, this approach to alloying aluminum with complex compounds leads to an improvement in the stability of mechanical properties at higher temperatures. The introduction of aluminum-magnesium spinel nanoparticles or silicon carbide nanoparticles enhances the mechanical properties of aluminum alloys and affects the motion of dislocations. In addition, because nanoparticles have a high surface energy, they can contribute to increasing the adhesive strength during aluminum particle sintering in small amounts. It should be noted that it is difficult to accurately assess the exact effect of these nanoparticles, especially spinel or silicon carbide. In the case of nanofilms of oxides present on aluminum nanoparticles and silicon carbide nanoparticles, their interaction is possible during spark plasma sintering and even the formation of aluminum oxycarbides is possible [37].

The difficulty in predicting each contribution is due to the fact that the SPS consolidation method is extremely non-equilibrium from a thermodynamic point of view, comprising the diffusion of atoms caused by different driving forces, namely thermal and electrical [38–40]. Furthermore, the formation of metastable states of phases can occur when high heating and cooling rates are employed, rendering the predictions of equilibrium thermodynamics inapplicable. Subsequent studies will address this issue from the perspective of nonlinear dynamics and kinetics.

In Al + Cr + Zr + Co + Ti + Cu system, at room temperature the optimal results were observed for a sample lacking nanoparticles, while at elevated temperatures, the Al + Cr + Zr + Co + Ti + Cu + 0.1SiC composite exhibited the most favorable outcomes. The incorporation of SiC nanoparticles along the grain boundaries can facilitate the reduction of creep along these boundaries by exerting pressure on the matrix and undergoing rotation during movement. Furthermore, as previously observed in analogous ternary systems [2], the presence of nanoparticles serves to reinforce the structural integrity of the compressed material, impeding the migration of defects and the coarsening of grains. This phenomenon exerts a beneficial influence on the strength of the material at elevated temperatures.

Conclusion

The bending strength of the composite Al – 0.5%Cr – 0.3%Zr – 0.2%Co – 0.2%Ti – 0.2%Cu reaches 335 MPa, while the Young's modulus is 76 GPa at 25 °C. At a temperature of 400 °C, the bending strength is 124 MPa, while the Young's modulus is 62 GPa. The material with the addition of 0.1 wt.% of SiC nanoparticles had an ultimate strength at 25 °C reaching 273 MPa, and at 400 °C of 191 MPa.

The addition of small amounts of alloying elements to aluminium forms intermetallic compounds that help reduce the grain size during sintering by preventing recrystallization. Additionally, the use of microadditives such as silicon carbide nanoparticles and aluminium magnesium spinels strengthens the aluminium structure. It has been shown that silicon carbide nanoparticles dissolve in aluminium, forming aluminium carbide, free silicon, and a small amount of a solid solution of silicon in aluminium, consistent with thermodynamic calculations.

Funding

This research was funded by the Ministry of Science and Higher Education of the Russian Federation in the framework of the "Goszadanie", grant number FSFF-2023–0006.

Acknowledgments

The authors would like to acknowledge the support received by the employees of the Department of Nanotechnology of JSC "Keldysh Research Center" for assistance in the research and valuable advice.

References

1. Prosviryakov A. S., Bazlov A. I., Bazlov A. I., Kishchik M. S., Mikhaylovskaya A. V. Microstructure and Mechanical Properties of Al – Cu – Mn Alloy Mechanically Alloyed with 5 wt% Zr After Multi-Directional Forging. *Metals and Materials International*. 2024. DOI: 10.1007/s12540-024-01800-y

2. Agureev L. E., Savushkina S. V., Laptev I. N., Ivanov A. V. Structure and Properties of Sintered Al – Cr – Zr Alloy. *Journal of Physics: Conference Series*. 2019. Vol. 1396. 012001.

3. Brodova I. G., Shirinkina I. G., Antonova O. V. Phase and Structural Transformations in the Al – Cr – Zr Alloy After

Rapid Melt Quenching and High-Pressure Torsion. *The Physics of Metals and Metallography*. 2007. Vol. 104, Iss. 3. pp. 281– 288.

4. Sytschev A. E., Lazarev P. A., Bogatov Yu. V., Boyarchenko O. A Study of the Structure and Properties of a Ti – Al – Mg/Ti-Based Metal–Intermetallic Material Produced by Self-Propagating High-Temperature Synthesis Combined with Pressing. *Inorganic Materials: Applied Research*. 2024. Vol. 5. pp. 1421–1428.

5. Nikolaev A., Ramazanov K., Nazarov A., Mukhamadeev V., Zagibalova E., Astafurova E. TEM Study of a Layered Composite Structure Produced by Ion-Plasma Treatment of Aluminum Coating on the Ti – 6Al – 4V Alloy. *Journal of Composites Science*. 2023. Vol. 7, Iss. 7. 271.

6. Popova E. A., Kotenkov P. V., Gilev I. O. Manifestation of Isomorphism in the Formation of Aluminides in Al Alloys with Two Transition Metals. *Inorganic Materials*. 2021. Vol. 57, Iss. 3. pp. 241–248.

7. Belov N. A. Phase Composition of Industrial and Advanced Aluminum Alloys. Moscow: Izdatelskiy dom "MISiS", 2010. 511p.

8. Muradyan G. N., Dolukhanyan S. K., Aleksanyan A. G., Ter-Galstyan O. P., Mnatsakanyan N. L. Regularities And Mechanism of Formation of Aluminides in the TiH_2– ZrH_2 – Al System. *Russian Journal of Physical Chemistry B*. 2019. Vol. 13, Iss. 1, pp. 86–95.

9. Popova E., Kotenkov P., Shubin A., Gilev I. Formation of Metastable Aluminides in Al – Sc – Ti (Zr, Hf) Cast Alloys. *Metals and Materials International*. 2020. Vol. 26. pp. 1515–1523.

10. Kotenkov P. V., Popova E. A., Gilev I. O. Influence of Small Additions of Ti and Zi on the Structure and Properties of the Al – 4%Cu Alloy. *Himicheskaya Fizika i Mezoskopiya*. 2019. Vol. 21, Iss. 1. pp. 23–28.

11. Tsunekawa S., Fine M. E. Lattice Parameters of $Al_3(Zr_xTi_{1-x})$ vs. x in Al – 2at.%(Ti + Zr) Alloys. *Scripta Metallurgica*. 1982. Vol. 16, Iss. 4. pp. 391–392.

12. Parameswaran V. R., Weertman J. R., Fine M. E. Coarsening Behavior of L12 Phase in an Al – Zr – Ti Alloy. *Scripta Metallurgica*. 1989. 23. pp. 147–150.

13. Lekatou A. G., Sfikas A. K., Karantzalis A. E. The Influence of the Fabrication Route on the Microstructure and Surface Degradation Properties of Al Reinforced by Al_9Co_2. *Materials Chemistry and Physics*. 2017. Vol. 200. pp. 33–49.

14. Deng Z.-X., Zhao D.-P., Huang Y.-Y., Chen L.-L., Zou H., Jiang Y., Chang K. Ab initio and CALPHAD-Type Thermodynamic Investigation of the Ti – Al – Zr System. *Journal of Mining and Metallurgy, Section B: Metallurgy*. 2019. Vol. 55, Iss. 3. pp. 427–437.

15. Boyer R., Welsch G., Collings E. W. Materials Properties Handbook: Titanium Alloys. ASM International, 1994. 1176 p.

16. Imayev V. M., Imayev R. M., Oleneva T. I. Current Status of γ-TiAl Intermetallic Alloys Investigations and Prospects for the Technology Developments. *Letters on Materials*. 2011. Vol. 1, Iss. 1. pp. 25–31.

17. Advanced Light Alloys and Composites. Ed. by R. Ciach. NATO Science Partnership Subseries: 3, 59. 1998. 534 p.

18. Mihalkovič M., Widom M. First-Principles Calculations of Cohesive Energies in the Al – Co Binary Alloy System. *Physical Review B*. 2007. Vol.75, Iss. 1. 014207.

19. Aubakirova R. K., Mansurov Yu. N., Sukurov B. M., Ibraeva G. M. Multilayer Structure of Intermetallic Compounds in the Diffusion Zone of the Al – Co System. *Kompleksnoe Ispol'zovanie Mineral'nogo Syr'ya*. 2018. No. 1. pp. 59–64.

20. Elagin V. I. Ways of Developing High-Strength and High-Temperature Structural Aluminum Alloys in the 21st Century. *Metal Science and Heat Treatment*. 2007. Vol. 49, Iss. 9-10, pp. 427–434.

21. Gobalakrishnan B., Rajaravi C., Udhayakumar G., Lakshminarayanan P. R. A Comparative Study on Ex-Situ & In-Situ Formed Metal Matrix Composites. *Archives of Metallurgy and Materials*. 2023. Vol. 68, Iss. 1. pp. 171–185.

22. Mironov V. V., Agureev L. E., Eremeeva Z. V., Kostikov V. I. Effect of Small Additions of Alumina Nanoparticles on the Strength Characteristics of an Aluminum Material. *Doklady Physical Chemistry*. 2018. Vol. 481, Iss. 2. pp. 110–113.

23. Lurie S., Volkov-Bogorodskiy D., Solyaev Y., Rizahanov R., Agureev L. Multiscale Modelling of Aluminium-Based Metal-Matrix Composites with Oxide Nanoinclusions. *Computational Materials Science*. 2016. Vol. 116. pp. 62–73.

24. Saunders N., Guo U. K. Z., Li X., Miodownik A. P., Schillé J.-P. Using *JMat*Pro to Model Materials Properties and Behavior. *JOM*. 2003. Vol. 55, Iss. 12. pp. 60–65.

25. Belov G. V., Trusov B. G. Thermodynamic Modeling of Chemically Reacting Systems: Moscow: Bauman Moscow State Technical University, 2013. 96 p.

26. Foadian F., Soltanieh M., Adeli M., Etminanbakhsh M. A Study on the Formation of Intermetallics During the Heat Treatment of Explosively Welded Al – Ti Multilayers. *Metallurgical and Materials Transactions A*. 2014. Vol. 45. pp. 1823– 1832.

27. Zhang C.-L., Wang X.-J., Wang X.-M., Hu X.-S., Wu K. Fabrication, Microstructure and Mechanical Properties of Mg Matrix Composites Reinforced by High Volume Fraction of Sphere TC4 Particles. *Journal of Magnesium and Alloys*. 2016. Vol. 4, Iss. 4. pp. 286–294.

28. Leszczyńska-Madej B., Garbiec D., Madej M. Effect of Sintering Temperature on Microstructure and Selected Properties of Spark Plasma Sintered Al – SiC composites. *Vacuum*. 2019. Vol. 164. pp. 250–255.

29. Sergeenko S. N., Alabid N. S. Hot-Deformed Powder Materials Based on Mechanochemically Activated Charges Al – SiC. *Tsvetnye Metally*. 2016. No. 9. pp. 68–77.

30. Kurbatkina E. I., Kosolapov D. V., Gololobov A. V., Shavnev A. A. Study on the Structure and Properties of Al – Zn – Mg – Cu/SiC Composite. *Tsvetnye Metally*. 2019. No. 1. pp. 40–45.

31. Urena A., Escalera M., Gil L. Oxidation Barriers on SiC Particles for Use in Aluminium Matrix Composites Manufactured by Casting Route: Mechanisms of Interfacial Protection. *Journal of Materials Science*. 2002. Vol. 37. pp. 4633–4643.

32. Baker A. G. Study of Mechanical and Physical Properties for SiC/Al Composites. *International Journal of Advances in Applied Science*. 2013. Vol. 2, Iss. 2. pp. 67–72.

33. Abedi M., Moskovskikh D., Nepapushev A., Suvorova V., Wang H., Romanovski V. Advancements in Laser Powder Bed Fusion of Carbon Nanotubes-Reinforced AlSi10Mg Alloy: A Comprehensive Analysis of Microstructure Evolution, Properties, and Future Prospects. *Metals*. 2023. Vol. 13. 1619.

34. Agureev L. E., Kostikov V. I., Yeremeyeva Z. V., Barmin A. A., Rizakhanov R. N., Ivanov B. S., Ashmarin A. A., Laptev I. N., Rudshteyn R. I. Powder Aluminum Composites of Al – Cu System with Micro-Additions of Pxide Nanoparticles. *Inorganic Materials: Applied Research*. 2016. Vol. 7, Iss. 5. pp. 687–690.

35. Agureev L. E., Laptev I. N., Ivanov B. S. et al. Development of Heat Resistant Aluminum Composite with Minor Addition of Alumina Nanofibers (Nafen™). *Inorganic Materials: Applied Research*. 2020. Vol. 11. pp. 1045–1050.

36. Poovazhagan L., Kalaichelvan K., Rajadurai A., Senthilvelan V. Characterization of Hybrid Silicon Carbide and Boron Carbide Nanoparticles-Reinforced Aluminum Alloy Composites. *Procedia Engineering*. 2013. Vol. 64. pp. 681–689.

37. Podrabinnik P., Gershman I., Mironov A., Kuznetsova E., Peretyagin P. Tribochemical Interaction of Multicomponent Aluminum Alloys During Sliding Friction with Steel. *Lubricants*. 2020. Vol. 8, Iss. 3. 24.

38. Monchoux J.-P. Sintering Mechanisms of Metals Under Electric Currents. *Spark Plasma Sintering of Materials*. 2019. pp. 93–115.

39. Dudina D. V., Georgarakis K., Olevsky E. A. Progress in Aluminium and Magnesium Matrix Composites Obtained by Spark Plasma, Microwave and Induction Sintering. *International Materials Review*. 2023. Vol. 68, Iss. 2. pp. 225–246.

40. Shkodich N. F., Rogachev A. S., Mukasyan A. S., Moskovskikh D. O., Kuskov K. V., Schukin A. S., Khomenko N. Y. Preparation of Copper–Molybdenum Nanocrystalline Pseudoalloys Using a Combination of Mechanical Activation and Spark Plasma Sintering Techniques. *Russian Journal of Physical Chemistry B*. 2017. Vol. 11, Iss. 1. pp. 173–179. NFM